Theory of nanorod antenna resonances including end-reflection phase

Wei Su,[1,2] Xiangyin Li,[1] Jens Bornemann,[2] and Reuven Gordon[2,*]

[1]*Nanophotonic and Metamaterial Laboratory, Department of Physics, Nanjing University of Science and Technology, Nanjing 210094, China*

[2]*Department of Electrical and Computer Engineering, University of Victoria, Victoria, British Columbia, Canada V8W 3V6*

(Received 27 November 2014; published 1 April 2015)

We present a fully analytic theory for nanorod resonances including the phase of reflection from the rounded ends using a transmission line approach. It combines the circuit theory response of spherical nanoparticles with standard transmission line theory using the Sommerfeld wave dispersion. The approach agrees well with comprehensive numerical calculations.

DOI: 10.1103/PhysRevB.91.165401 PACS number(s): 73.20.Mf, 78.67.Qa

I. INTRODUCTION

Nanorods are of great interest in plasmonics for their application to surface enhanced Raman spectroscopy [1], antennas [2], solar cells [3,4], nonlinear optics [5,6], sensing [7–10], and imaging [11,12]. Colloidal nanorods can be wavelength tuned by variations to their diameter and length [13]. A previous work has proposed a theory for the resonant wavelength of the antenna scaling in the visible regime by using the Sommerfeld wave dispersion [14]. That work set the reflection phase equal to zero at the transition to the round end of the nanorod, although accurate solutions require accounting for the finite phase [15]. For flat end nanorods, other works have shown a nonzero reflection phase that can be calculated analytically [16–18], and these have been used to model accurately the resonance response [19]. For rounded end nanorods, numerical calculations have shown that the reflection phase is nonzero [20] and actually strongly dispersive over the visible near-IR regime. For nanoantenna design, it is highly desirable to have a fully analytic theory to calculate the nanorod resonances for rounded ends naturally occurring for colloidal samples.

Here we use a circuit theory approach for nanoparticles to solve for the nanorod resonances. Our approach combines the circuit theory response of spherical nanoparticles [21,22] with standard transmission line theory [23] using the Sommerfeld wave dispersion [24]. We find a fully analytic theory for the reflection phase and compare with comprehensive numerical calculations.

II. CIRCUIT THEORY FOR NANORODS

Figure 1(a) shows the schematic of a nanorod, where r is the radius of the nanorod and L is the length from end to end. Figure 1(b) shows the equivalent circuit of the nanorod. According to Ref. [21], we know that a nanosphere of radius r made of noble metals (e.g., Ag, Au) can be treated as a circuit "lumped nanoelement." Considering an electromagnetic wave E_0 illuminating the sphere, the fields inside and outside the sphere can be equivalent to three displacement currents, I_{imp}, I_{sph}, and I_{fringe}, which represent the impressed displacement current source, the displacement current circulating in the nanosphere, and the displacement current of the fringe field, respectively. Here, we consider the material of the sphere to be metal, so the equivalent circuit for the optical wave interaction with a sphere can be presented as the blue rectangular part in Fig. 1(b). The impedances can be written as [21]

$$Z_{\text{sph}} = (-i\omega\varepsilon_0\varepsilon_m\pi r)^{-1}, \quad Z_{\text{fringe}} = (-i\omega 2\pi r\varepsilon_0\varepsilon_d)^{-1}, \quad (1)$$

where $\varepsilon_m = \varepsilon_m' + i\varepsilon_m''$ is the nanorod's material permittivity, r is the radius, ε_d is the permittivity of the dielectric medium surrounding the nanorod, and ε_0 is the background permittivity.

For rounded end nanorods, when the plasmonic resonance for the optical wave interacts with the nanorod, we can treat the nanorod as a cylinder plus a sphere. According to transmission line theory, we can treat the cylinder as a transmission line with impedance Z_S, and regard the right part in Fig. 1(b) as a load, with impedance Z_L. So we can get the reflection Γ from [25]

$$\Gamma = \frac{Z_L - Z_S}{Z_L + Z_S}, \quad (2)$$

where

$$Z_S = \sqrt{\frac{\mu_0}{\varepsilon_0}}\frac{k_0}{\beta}, \quad (3)$$

$$\frac{1}{Z_L} = \frac{1}{Z_{\text{sph}}} + \frac{1}{Z_{\text{fringe}}}. \quad (4)$$

Here, μ_0 is the background permeability, k_0 is the free-space wave vector, and β is the propagation constant in the nanorod.

So, we can obtain the phase of the reflection Φ as

$$\Phi = \text{angle}\,[\Gamma]\,. \quad (5)$$

III. DISCUSSION AND CALCULATIONS

Figure 2 shows the phase of reflection as a function of wavelength for different ε_d; the nanorod has a radius of 10 nm, and silver (Ag) is used as the metal, with its dispersive permittivity fully considered [26]. It can be seen that at long wavelengths, the phase tends to a constant value, which suggests a perfect metal-like behavior. The dashed lines, extracted for comparison from Fig. 3 of Ref. [20], are from the simulation of a semi-infinite wire for the respective lowest order propagating surface plasmon polariton mode, i.e., the Sommerfeld surface wave. The solid lines show the data calculated by Eq. (2).The analytic theory shows reasonable agreement with the comprehensive simulations of Ref. [20].

*Corresponding author: rgordon@uvic.ca

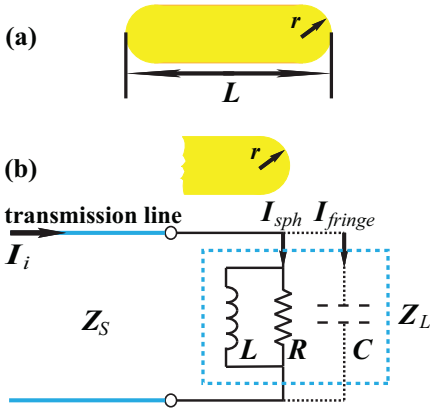

FIG. 1. (Color online) (a) A schematic of a nanorod. (b) Its equivalent circuit.

Here, we compare the theory with comprehensive finite-difference time-domain (FDTD) simulations of the resonances of nanorods of varying size. Gold (Au) is used as the metal, the relative permittivity values for gold are taken from experimental measurements [26], the refractive index of the dielectric medium surrounding the nanorod is 1.33, and the nanorod has a diameter of 25 nm.

Figure 3 shows the resonant wavelength as a function of nanorod length. The results show the linear relationship between the resonant wavelength and the nanorod length. The resonant wavelengths calculated with FDTD show a good agreement with the analytic theory.

According to the cylindrical waveguide theory, we can get the propagation constant of the Sommerfeld surface wave β in the nanorod by [16]

$$\frac{K_0(p_d r)\, I_1(p_m r)}{K_1(p_d r)\, I_0(p_m r)} = -\frac{\varepsilon_d p_m}{\varepsilon_m p_d}, \tag{6}$$

with I_n and K_n being the modified Bessel functions of first and second kind of order n, where $p_{m,d} = \sqrt{\beta^2 - k_0^2 \varepsilon_{m,d}}$, $\varepsilon_{m,d}$ are the relative permittivities of the metal and dielectric, $k_0 = \omega/c$, c is the speed of light in free space, ω is the angular frequency of the electromagnetic wave corresponding to the

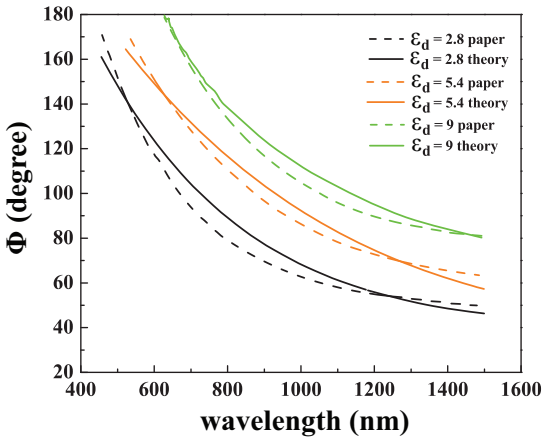

FIG. 2. (Color online) Phase of the reflection Φ of the nanorod for selected values of ε_d : $\varepsilon_d = 2.8$ (black), $\varepsilon_d = 5.4$ (orange), and $\varepsilon_d = 9$ (green). The solid lines show the data calculated by Eq. (2) and the dashed lines show the data from Ref. [20].

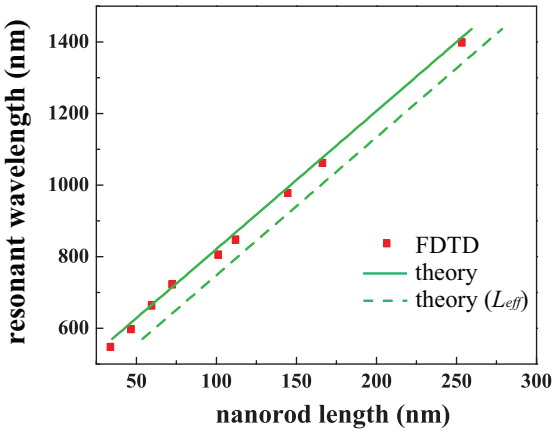

FIG. 3. (Color online) Resonant wavelengths of 25 nm diameter nanorods for different lengths. Red dots correspond to resonant wavelengths calculated with FDTD, the green solid line corresponds to the results from analytic theory, and the green dotted line corresponds to the results if we assume $\Phi = 0$.

resonant wavelength, and r is the cylinder radius. Considering the propagation of the surface wave along the rod and reflection at the ends, we can calculate the Fabry-Pérot resonances of a nanorod,

$$\beta(L - 2r) + \Phi = m\pi, \tag{7}$$

where m is the whole-number resonance order.

In the past, an effective rod length L_{eff} was given by subtracting the ends and setting $\Phi = 0$ [14],

$$\beta L_{\text{eff}} = m\pi. \tag{8}$$

So, according to Eqs. (7) and (8), we can obtain the relationship between L_{eff} and the resonant wavelength, as shown by the dotted line in Fig. 3. There still exists a shift between the theory presented here and this effective length scaling. It is possible to define a new effective length L'_{eff} based on the best fit to the theory while still assuming $\Phi = 0$. In this case, we find that $L'_{\text{eff}} = 1.2(L - 2r) = 1.2L_{\text{eff}}$. Therefore, an accurate effective length scaling is possible, as noted in Ref. [14]; however, the length should be revised to account for the finite phase of reflection at the rod ends.

Figure 4 shows the phase of reflection as a function of wavelength from both comprehensive numerical calculations and circuit theory for three different diameter nanorods. The differences are less than 10°. Overall, we find good agreement in the predicted phases by both methods.

The phase of reflection of the semi-infinite waveguide agrees with the phase for a finite waveguide. This is an interesting result, which implies that the fields on either side of the waveguides do not significantly influence each other. We have seen good agreement between numerical simulations of the finite rods and the theory based on the semi-infinite rods even for cases $(L - 2r) < 2r$. For example, for a rod of diameter 25 nm, we saw good agreement for $(L - 2r) = 9$ nm.

The quasistatic approximation applies for small particles ($r \ll \lambda$). In this case, the phase of the electromagnetic field is almost constant in the local region. Therefore, we can treat the responses of the optical field at the nanorod ends without retardation. Equation (1) is only valid within the

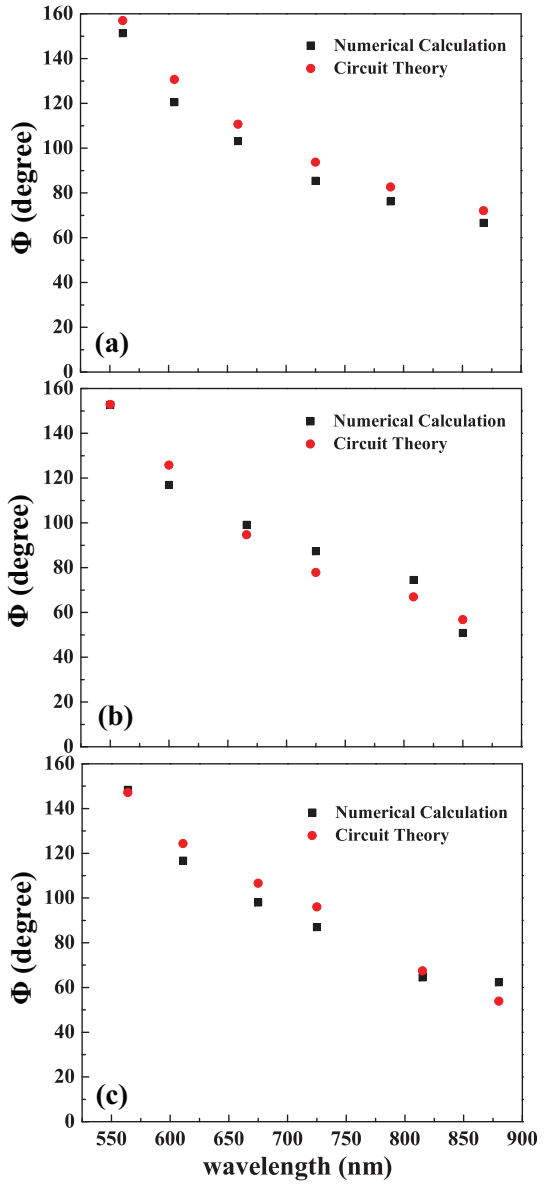

FIG. 4. (Color online) Phases of the reflection Φ as a function of wavelengths for (a) 20, (b) 25, and (c) 30 nm diameter nanorods.

quasistatic approximation and this also ensures a single channel matching for Eq. (4). For larger diameters, these results will no longer be valid. So, for larger nanorods, the quasistatic approximation would break down due to retardation effects [27]. We have tested this breakdown by increasing the diameter of the nanorods for a constant resonance wavelength of 700 nm (scaling the geometry accordingly) and found that the variation in the phase between the analytic theory and FDTD computation begins to exceed 10° when the diameter of the nanorod is larger than 70 nm.

Figure 5 shows a image map of the phase shift difference between the theory and simulation, as a function of nanorod diameter and $(L - 2r)$. As described above, this figure shows that when the nanorod diameter exceeds 70 nm, the theory becomes inaccurate (i.e., it departs from the comprehensive simulation results), which shows the breakdown of the quasistatic approximation for this size.

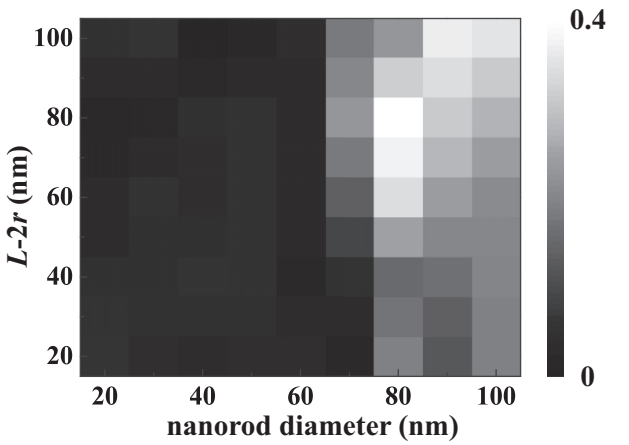

FIG. 5. Phase shift between the theory and simulation results as a function of nanorod diameter and $(L - 2r)$. The grayscale shows the value of $(\Phi_{\text{theory}} - \Phi_{\text{simulation}})/\pi$.

The length of the nanorods does not physically limit the theory since it includes the retardation from propagation and is not limited by quasistatic assumptions. Indeed, the theory can be applied to higher order resonances and we have extended this to $L \gg 2r$. For example, for a rod of diameter 25 nm, we saw good agreement for $(L - 2r) = 143$ nm. In practice, however, losses along the rod will limit the strength of the resonances for longer rods.

We next consider the width of the resonance peak. Considering the propagation loss in the nanorod, the quality factor of the circuit Q can be written from Fabry-Pérot analysis as

$$\frac{1}{Q} = 1 - e^{-4\beta''(L-2r)}|\Gamma|^2, \tag{9}$$

where β'' is the imaginary part of β.

So, the bandwidth B is

$$B = \frac{\omega_0}{Q}, \tag{10}$$

where ω_0 is the resonant frequency.

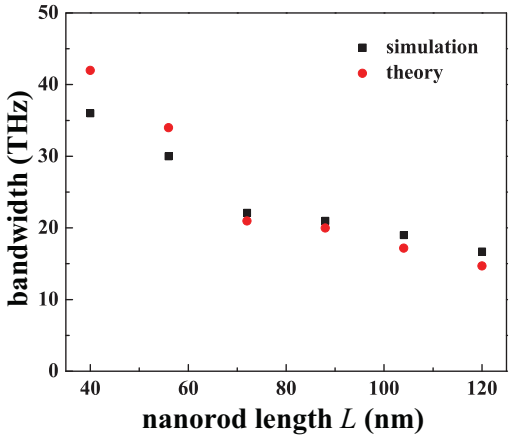

FIG. 6. (Color online) Bandwidths of the resonance peak as a function of nanorod length. The diameter of the nanorods is 30 nm.

Figure 6 shows the bandwidth as a function of nanorod length. Good agreement is found between the simulation results and the values calculated from Eq. (10).

IV. CONCLUSIONS

In conclusion, we have presented a fully analytic theory for nanorod resonances including the phase of reflection from the rounded ends by using a transmission line approach combined with a nanocircuit theory of the rounded ends. The theory shows good agreement with calculations from past works as well as comprehensive numerical calculations presented here. This work will be useful in the rapid design of nanorod geometries to achieve desired resonance wavelengths. Furthermore, it is possible to envision extending this approach to more generalized scenarios, such as ellipsoidal end faces, or coupled nanorods.

ACKNOWLEDGMENT

This work was supported by research funding from the Chinese Scholarship Council and Natural Sciences and Engineering Research Council (NSERC) Canada Discovery Grants program.

APPENDIX: FDTD SIMULATIONS

In this paper, the nanorods were simulated by the finite-difference time-domain (FDTD) method (Lumerical FDTD 8.1). Polarization of the incident field was parallel to the long nanorod axis. The simulation domain was terminated with perfectly matched layers. The complex permittivity of the metal was modeled using the experimental data of Johnson and Christy [26]. To calculate the cross sections of the nanorods, we employed the formalism of the total field scattered field (TFSF). We introduced a set of two-dimensional power monitors, which formed two surfaces enclosing the nanorods: one inside the TF region (monitor 1) and the other one in the SF region (monitor 2). We calculated the absorption cross section of the nanostructures by evaluating the net power flow into monitor 1. The total power exiting monitor 2 was used for the calculation of the scattering cross section. The extinction cross section was determined by the summation of scattering and absorption cross sections.

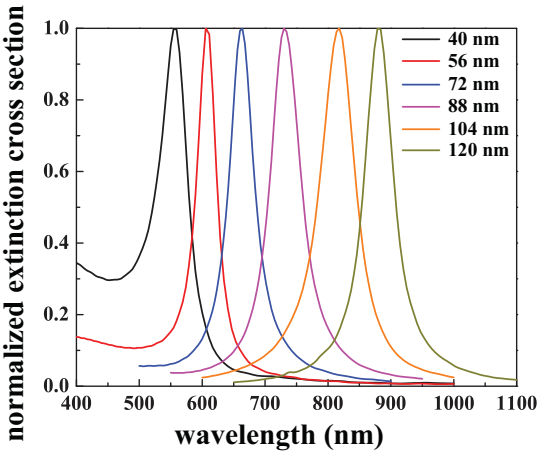

FIG. 7. (Color online) Normalized extinction cross sections as a function of wavelength for various nanorod lengths. The diameter of the nanorods is 30 nm.

Figure 7 shows the normalized extinction cross sections as a function of wavelength for various nanorods lengths from 40 to 120 nm. The diameter of the nanorods is 30 nm. According to the peaks, we can obtain the locations of the resonant wavelengths.

[1] J. Kumar and K. G. Thomas, Surface-enhanced raman spectroscopy: Investigations at the nanorod edges and dimer junctions, J. Phys. Chem. Lett. **2**, 610 (2011).

[2] J. Dorfmüller, R. Vogelgesang, W. Khunsin, C. Rockstuhl, C. Etrich, and K. Kern, Plasmonic nanowire antennas: Experiment, simulation, and theory, Nano Lett. **10**, 3596 (2010).

[3] J. H. Bang and P. V. Kamat, Solar cells by design: Photoelectrochemistry of TiO_2 nanorod arrays decorated with CdSe, Adv. Funct. Mater. **20**, 1970 (2010).

[4] M. Wu, X. Lin, A. Hagfeldtb, and T. Ma, A novel catalyst of WO_2 nanorod for the counter electrode of dye-sensitized solar cells, Chem. Commun. **47**, 4535 (2011).

[5] G. A. Wurtz, R. Pollard, W. Hendren, G. P. Wiederrecht, D. J. Gosztola, V. A. Podolskiy, and A. V. Zayats, Designed ultrafast optical nonlinearity in a plasmonic nanorod metamaterial enhanced by nonlocality, Nat. Nanotechnol. **6**, 107 (2011).

[6] H. Baida, D. Mongin, D. Christofilos, G. Bachelier, A. Crut, P. Maioli, N. Del Fatti, and F. Vallée, Ultrafast nonlinear optical response of a single gold nanorod near its surface plasmon resonance, Phys. Rev. Lett. **107**, 057402 (2011).

[7] J. Becker, A. Trügler, A. Jakab, U. Hohenester, and C. Sönnichsen, The optimal aspect ratio of gold nanorods for plasmonic bio-sensing, Plasmonics **5**, 161 (2010).

[8] J. Yi, J. M. Lee, and W. I. Park, Vertically aligned ZnO nanorods and graphene hybrid architectures for high-sensitive flexible gas sensors, Sens. Actuators, B **155**, 264 (2011).

[9] L. Vigderman, B. P. Khanal, and E. R. Zubarev, Functional gold nanorods: Synthesis, self-assembly, and sensing applications, Adv. Mater. **24**, 4811 (2012).

[10] K. M. Mayer and J. H. Hafner, Localized surface plasmon resonance sensors, Chem. Rev. **111**, 3828 (2011).

[11] B. Jang, J. Y. Park, C. H. Tung, I. H. Kim, and Y. Choi, Gold nanorod−photosensitizer complex for near-infrared fluorescence imaging and photodynamic/photothermal therapy in vivo, ACS Nano **5**, 1086 (2011).

[12] H.-G. Liao, L. K. Cui, S. Whitelam, and H. M. Zheng, Real-time imaging of Pt_3Fe nanorod growth in solution, Science **336**, 1011 (2012).

[13] S. Link, C. Burda, M. B. Mohamed, B. Nikoobakht, and M. A. El-Sayed, Femtosecond transient-absorption dynamics of

colloidal gold nanorods: Shape independence of the electron-phonon relaxation time, Phys. Rev. B **61**, 6086 (2000).

[14] L. Novotny, Effective wavelength scaling for optical antennas, Phys. Rev. Lett. **98**, 266802 (2007).

[15] T. H. Taminiau, R. J. Moerland, F. B. Segerink, L. Kuipers, and N. F. van Hulst, λ/4 Resonance of an optical monopole antenna probed by single molecule fluorescence, Nano Lett. **7**, 28 (2007).

[16] R. Gordon, Reflection of cylindrical surface waves, Opt. Express **17**, 18621 (2009).

[17] J. Dorfmüller, R. Vogelgesang, R. T. Weitz, C. Rockstuhl, C. Etrich, T. Pertsch, F. Lederer, and K. Kern, Fabry-pérot resonances in one-dimensional plasmonic nanostructures, Nano Lett. **9**, 2372 (2009).

[18] R. Kolesov, B. Grotz, G. Balasubramanian, R. J. Stöhr, A. A. L. Nicolet, P. R. Hemmer, F. Jelezko, and J. Wrachtrup, Wave-particle duality of single surface plasmon polaritons, Nat. Phys. **5**, 470 (2009).

[19] S. B. Hasan, C. Etrich, R. Filter, C. Rockstuhl, and F. Lederer, Enhancing the nonlinear response of plasmonic nanowire antennas by engineering their terminations, Phys. Rev. B **88**, 205125 (2013).

[20] S. B. Hasan, R. Filter, A. Ahmed, R. Vogelgesang, R. Gordon, C. Rockstuhl, and F. Lederer, Relating localized nanoparticle resonances to an associated antenna problem, Phys. Rev. B **84**, 195405 (2011).

[21] N. Engheta, A. Salandrino, and A. Alù, Circuit elements at optical frequencies: Nanoinductors, nanocapacitors, and nanoresistors, Phys. Rev. Lett. **95**, 095504 (2005).

[22] J. S. Huang, T. Feichtner, P. Biagioni, and B. Hecht, Impedance matching and emission properties of nanoantennas in an optical nanocircuit, Nano Lett. **9**, 1897 (2009).

[23] G. Goubau, Surface waves and their application to transmission lines, J. Appl. Phys. **21**, 1119 (1950).

[24] A. Sommerfeld, Ueber die fortpflanzung elektrodynamischer wellen längs eines drahtes, Ann. Phys. Chem. **303**, 233 (1899).

[25] F. T. Ulaby, *Electromagnetics for Engineers* (Prentice Hall, Upper Saddle River, NJ, 2004).

[26] P. B. Johnson and R. W. Christy, Optical constants of the noble metals, Phys. Rev. B **6**, 4370 (1972).

[27] S. A. Maier, *Plasmonics: Fundamentals and Applications* (Springer, New York, 2007).